

## Suppression and Regression of Choroidal Neovascularization by Systemic Administration of an $\alpha_5\beta_1$ Integrin Antagonist

Naoyasu Umeda, Shu Kachi, Hideo Akiyama, Grit Zahn, Doerte Vossmeier, Roland Stragies, Peter A. Campochiaro

The Departments of Ophthalmology and Neuroscience  
The Johns Hopkins University School of Medicine  
Maumenee 719  
600 N. Wolfe Street  
Baltimore, Maryland 21287-9277      NU, HA, PAC

<sup>2</sup>Jerini Pharmaceuticals  
Berlin, Germany      GZ, DV, RS

## Running Title: $\alpha_5\beta_1$ Integrin and Ocular Neovascularization

Supported by the Foundation Fighting Blindness, the Macula Vision Foundation, and EY12609 from the NEI. PAC is the George S. and Dolores Dore Eccles Professor of Ophthalmology.

Address correspondence to: Peter A. Campochiaro, M.D.  
Maumenee 719  
The Johns Hopkins University School of Medicine  
600 N. Wolfe Street  
Baltimore, MD 21287-9277  
Telephone #: (410) 955-5106  
Fax #: (410) 614-9315  
Email: [pcampo@jhmi.edu](mailto:pcampo@jhmi.edu)

Text pages- 21  
Tables- 0  
Figures- 6  
References- 28  
Abstract- 155  
Introduction- 495  
Discussion- 716

Abbreviations- hypoxia-inducible factor-1 (HIF-1), vascular endothelial growth factor (VEGF), extracellular matrix (ECM), phosphate-buffered saline (PBS), Tris-buffered saline (TBS), terminal deoxynucleotidyl transferase-mediated dUTP-FITC nick-end labeling (TUNEL), extracellular signal regulated kinase (ERK) fluorescent activated cell sorting (FACS), outer nuclear layer (ONL), Human umbilical vein endothelial cells (HUVEC), fibroblast growth factor 2 (FGF2), tumor necrosis factor- $\alpha$  (TNF- $\alpha$ ), or interleukin-8 (IL-8), age-related macular degeneration (AMD), *Griffonia simplicifolia* lectin (GSA), focal adhesion kinase (FAK),

## Abstract

Integrin  $\alpha_5\beta_1$  plays an important role in developmental angiogenesis, but its role in various types of pathologic neovascularization has not been completely defined. In this study, we found strong upregulation of  $\alpha_5\beta_1$  in choroidal neovascularization. Implantation of an osmotic pump delivering 1.5 or 10  $\mu\text{g}/\text{hour}$  ( $\sim 1.8$  or 12  $\text{mg}/\text{kg}/\text{day}$ ) of JSM6427, a selective  $\alpha_5\beta_1$  antagonist, caused significant suppression of choroidal neovascularization; the area of neovascularization was reduced by 33 to 40%. When an osmotic pump delivering 10  $\mu\text{g}/\text{hour}$  of JSM6427 was implanted 7 days after rupture of Bruch's membrane, there was TUNEL staining in vascular cells within the neovascularization and significant regression of the neovascularization over the next week. JSM6427 also induced apoptosis of cultured vascular endothelial cells. Fibronectin stimulates phosphorylation of extracellular signal regulated kinase (ERK) in  $\alpha_5\beta_1$ -expressing cells and this is blocked by JSM6427. These data suggest that  $\alpha_5\beta_1$  plays a role in the development and maintenance of choroidal neovascularization and provides a target for therapeutic intervention.

## Introduction

Vascular endothelial cells participating in angiogenesis get signals from several sources. Surrounding tissue that senses the need for increased blood (oxygen) delivery is an important source of soluble stimulators. In hypoxic tissue, the transcription factor, hypoxia inducible factor-1 (HIF-1) is stabilized, resulting in upregulation of several genes (Manalo et al., 2005). Vascular endothelial growth factor (VEGF) is an important hypoxia-regulated soluble signal produced by surrounding tissue that promotes neovascularization. Things other than hypoxia, such as cytokines, also up-regulate VEGF, and in many instances this appears to be through HIF-1 or HIF-2 (Bardos et al., 2004; Haddad and Harb, 2005). While other soluble signals undoubtedly play a role, it is clear that inhibition of VEGF is a useful strategy for treatment of neovascular diseases (Ribatti, 2005).

Another source of signals is the extracellular matrix (ECM). The ECM seems capable of providing both stabilizing signals that suppress neovascularization and stimulatory signals (Sottile, 2004). Integrins are cell surface receptors that mediate signaling from the ECM and one way that signaling from ECM is modulated is by alterations in the integrin population on the cell surface. Therefore, it is important to determine in any given situation, which integrins mediate stimulation of neovascularization and which seem to suppress it.

Integrins  $\alpha_v\beta_3$  and  $\alpha_v\beta_5$  are up-regulated on endothelial cells participating in several types of neovascularization, including tumor vessels and retinal neovascularization (Brooks et al., 1994a; Brooks et al., 1994b; Luna et al., 1996). Antagonists of  $\alpha_v\beta_3$  and  $\alpha_v\beta_5$  suppress tumor neovascularization and retinal neovascularization (Hammes et al., 1996; Luna et al., 1996). However, the same antagonists of  $\alpha_v\beta_3$  and  $\alpha_v\beta_5$  that suppress retinal neovascularization, have no identifiable suppressive effect on choroidal neovascularization in mice (unpublished data). Gene knockout studies have shown that deletion of  $\alpha_v$ ,  $\beta_3$ , and/or  $\beta_5$  fails to block developmental angiogenesis and in some cases may enhance angiogenesis (Hynes, 2002). Therefore, it appears that the role of integrins in neovascularization in one situation does not guarantee participation in a different vascular bed and different disease process.

Integrin  $\alpha_5\beta_1$  is also up-regulated on activated endothelial cells and tumor blood vessels (Collo and Pepper, 1999; Kim et al., 2000; Magnussen et al., 2005; Parsons-Wingerter et al., 2005). Antagonists of  $\alpha_5\beta_1$  suppress angiogenesis on chick chorioallantoic membrane induced by FGF2, tumor necrosis factor- $\alpha$  (TNF- $\alpha$ ) or interleukin-8 (IL-8) and in murine tumor models (Kim et al., 2000; Magnussen et al., 2005; Stoeltzing et al., 2003). Integrin  $\alpha_5\beta_1$  also plays a critical role in developmental angiogenesis (Hynes, 2002; Yang et al., 1993). During vascularization of the central nervous system, angiogenic sprouts express high levels of  $\alpha_5\beta_1$  and it is markedly reduced as the vessels mature (Milner and Campbell, 2002). Thus,  $\alpha_5\beta_1$  appears to promote angiogenesis in multiple settings, but as noted above, one cannot assume that it is proangiogenic in all

tissues and pathologies. In this study, we have explored the role of  $\alpha_5\beta_1$  in choroidal neovascularization, the most common cause of severe vision loss in elderly Americans (Klein et al., 1993).

## Materials and Methods

### **Mouse model of choroidal neovascularization**

Mice were treated in accordance with the Association for Research in Vision and Ophthalmology guidelines for the use of animals in research. Choroidal neovascularization was induced by laser photocoagulation-induced rupture of Bruch's membrane as previously described (Tobe et al., 1998). Briefly, 5 to 6 week old female C57BL/6J mice were anesthetized with ketamine hydrochloride (100 mg/kg body weight), and pupils were dilated with 1% tropicamide. Three burns of 532 nm diode laser photocoagulation (75  $\mu$ m spot size, 0.1 seconds duration, 120 mW) were delivered to each retina with the slit lamp delivery system of an OcuLight GL diode laser (Iridex, Mountain View, CA) using a handheld cover slip as a contact lens to view the retina. Burns were performed in the 9, 12, and 3 o'clock positions of the posterior pole of the retina. Production of a bubble at the time of laser, which indicates rupture of Bruch's membrane, is an important factor in obtaining choroidal neovascularization, and therefore, only burns in which a bubble was produced were included in the study.

### **Immunohistochemistry and histochemistry**

Two weeks after rupture of Bruch's membrane, mice were euthanized and eyes were removed and fixed for 30 minutes in 0.1 M phosphate buffer, pH 7.6 containing 4% paraformaldehyde and 5% sucrose. After 30 minutes, corneas and lenses were removed and then fixation was continued for another hour.

After washing with 0.1 M phosphate buffer containing 20% sucrose overnight, the eyecups were frozen in optimum cutting temperature embedding compound (Miles Diagnostics, Elkhart, IN, USA). Ocular frozen sections (10  $\mu$ m) were dried with cold air for 20 minutes, fixed in freshly prepared 4% paraformaldehyde in 0.05 M phosphate-buffered saline (PBS) at room temperature for 15 minutes, and rinsed with 0.05 M Tris-buffered saline (TBS) for 10 minutes. Endogenous peroxidases were inhibited by a 15 minute incubation with 0.75% H<sub>2</sub>O<sub>2</sub> in methanol. Sections were washed 3 times in 0.05 M TBS and nonspecific-binding sites were blocked by incubating in 10% normal goat serum in 50 mM TBS for 30 minutes at room temperature. Sections were incubated with 1:200 rabbit polyclonal antibody directed against  $\alpha_5$  integrin subunit (AB1928, Chemicon, Temecula, CA, USA) in 1% bovine serum albumin (BSA) in TBS at 4°C overnight. For controls, non-immune IgG (Vector Laboratories, Burlingame, CA) was substituted for primary antibody. After 2 rinses with TBS, sections were incubated for 30 minutes at room temperature with secondary antibody, 1:1000 FITC-conjugated goat anti-rabbit IgG F(ab')<sub>2</sub> (111-096-006, Jackson ImmunoResearch, West Grove, PA). Sections were counterstained with DAPI (Kirkegaard and Perry, Gaithersburg, MD) and mounted with Aquamount (BDH, Poole, UK).

Serial sections were stained with biotinylated *Griffonia simplicifolia* lectin B4 (GSA, Vector Laboratories) to identify choroidal neovascularization as previously described (Ozaki et al., 1998). Briefly, slides were incubated in methanol/H<sub>2</sub>O<sub>2</sub> for 10 minutes at 4°C, washed with 0.05 M TBS, pH 7.6 and



incubated for 30 minutes in 10% normal porcine serum. Slides were incubated 2 hours at room temperature with biotinylated GSA. After washing, the slides were incubated in streptavidin-phosphatase and developed with HistoMark Red (Kirkegaard and Perry) according to the manufacturer's instructions. Sections were dehydrated and mounted with Cytoseal. Stained sections were examined with a Nikon microscope and captured as digital files with a Nikon DXM1200 Digital Still Camera (Nikon Instruments Inc., New York, NY).

### **Systemic administration of JSM6427 in mice with rupture of Bruch's membrane**

Two different concentrations of JSM6427, 3 mg/ml in PBS and 20 mg/ml in 100 mM glycine/NaOH, pH 4.0 or the corresponding vehicle alone were loaded into osmotic mini-pumps (model 2002; Alza Corp., Palo Alto, CA) with internal volume of 200  $\mu$ l and mean pumping rate of 0.5  $\mu$ l/h. Pumps were implanted beneath the skin of the back and the following day the mice had laser-induced rupture of Bruch's membrane at 3 locations in each eye. After 14 days, the mice were perfused with 1 ml of PBS containing 50 mg/ml of fluorescein-labeled dextran ( $2 \times 10^6$  average molecular weight, Sigma-Aldrich, St. Louis, MO) and choroidal flat mounts were prepared as previously described. Briefly, eyes were removed and fixed for 1 hour in 10% phosphate-buffered formalin. The cornea, lens, and retina were removed and four radial cuts were made in the eyecup allowing it to be flat mounted in aqueous mounting medium. Flat mounts were examined by fluorescence microscopy and images were digitized using a three-

color charge-coupled device video camera and a frame grabber. Image analysis software (Image-Pro Plus, Media Cybernetics, Silver Spring, MD) was used to measure the total area of choroidal neovascularization at each rupture site.

To assess the effect of JSM6427 on established choroidal neovascularization, mice had rupture of Bruch's membrane at 3 locations in each eye and after 7 days, 9 mice were perfused with fluorescein-labeled dextran and the baseline area of neovascularization at each rupture site was measured. The remaining mice had implantation of osmotic mini-pumps containing 20 mg/ml of JSM6427 in 100 mM Na phosphate buffer, 50 mM NaCl, pH 7.4 or vehicle alone. At 7 days after implantation some mice were euthanized for terminal deoxynucleotidyl transferase-mediated dUTP-FITC nick-end labeling (TUNEL). The remainder of the mice was perfused with fluorescein-labeled dextran 7 days after implantation and the area of choroidal neovascularization at rupture sites was measured.

### **Intravitreal injections of JSM6427**

Mice had rupture of Bruch's membrane at 3 locations in each eye and were given an intravitreal injection of 1  $\mu$ l of vehicle (PBS or 100 mM phosphate buffer, 50 mM NaCl, pH 7.4) containing of 3 or 20  $\mu$ g of JSM6427 in one eye and 1  $\mu$ l of vehicle alone in the other eye on days 0 and 7. For an additional control, some mice did not receive any injection. On day 14 the mice were perfused with fluorescein-labeled dextran and the area of choroidal neovascularization at Bruch's membrane rupture sites was measured.

### **Identification of apoptotic cells *in vivo* by TUNEL**

Eyes were fixed in 4% paraformaldehyde in 0.1 M phosphate buffer and frozen in OCT. Ten  $\mu\text{m}$  serial sections were cut through each rupture site. Sections were fixed with 1% paraformaldehyde for 10 minutes at room temperature and TUNEL was done with the ApopTag Red kit (S7165, Chemicon) according to the manufacturer's instructions. The sections were also histochemically stained with GSA as described above. Slides were also stained with DAPI and mounted in aqueous mounting medium.

### **Statistical analysis**

Data were analyzed using linear mixed model accounting for possible correlations in measurements from the same mice. Dunnett's adjustment was made for multiple comparisons.

### **Solid phase binding assay**

The inhibiting activity and integrin selectivity of the integrin inhibitor was determined in a solid phase binding assay using soluble integrins and coated extracellular matrix protein. Binding of integrins was then detected by specific antibodies in an enzyme-linked immunosorbant assay. Fibronectin and vitronectin were purchased from Sigma (St Louis, MO). The integrin  $\alpha_5\beta_1$  extracellular domain Fc-fusion protein was a generous gift from M. Humphries (University of Manchester) and  $\alpha_V\beta_3$  was purchased from Chemicon (Chemicon

Europe, Germany). The integrin antibodies were purchased from Pharmingen, BD Bioscience Europe ( $\alpha_v\beta_3$ ) and Sigma (anti-human-Fc-HRP antibody conjugate and anti-mouse-HRP conjugate).

The detection of HRP was performed using HRP substrate solution 3,3',5,5'-tetramethylethylenediamine (TMB, Seramun, Germany) and 1M H<sub>2</sub>SO<sub>4</sub> for stopping the reaction. The developed color was measured at 450nm.

$\alpha_5\beta_1$ : Nunc-Immuno maxisorp plates (Nalge Nunc Europe Ltd) were coated overnight at 4°C with fibronectin (0.25 µg/ml) in 15 mM Na<sub>2</sub>CO<sub>3</sub>, 35 mM NaHCO<sub>3</sub>, pH9.6. All subsequent washing and binding were performed in 25 mM Tris, pH7.6, 150 mM NaCl, 1 mM MnCl<sub>2</sub>, 1 mg/ml BSA. The plates were blocked with 3 % BSA in PBS 0.1 % Tween20 for 1 hour at room temperature. Soluble integrin  $\alpha_5\beta_1$  (0.5 µg/ml) and a serial dilution of integrin inhibitor were incubated in the coated wells for one hour at room temperature. The detection antibody (anti-human-Fc-HRP antibody conjugate) was then applied for 1 hour at room temperature and the binding visualized as described above. For the  $\alpha_v\beta_3$  assay, plates were coated with vitronectin (1 µg/ml) and blocked as described for  $\alpha_5\beta_1$ . Soluble  $\alpha_v\beta_3$  (1 µg/ml) was incubated with a serial dilution of integrin inhibitor for one hour at room temperature. Primary (anti- $\alpha_v\beta_3$ ) and secondary antibody (anti-mouse-HRP conjugate) were applied for 1 hour at RT and the binding visualized as described above. All IC<sub>50</sub> measurements were performed at least 30 times.

### **Identification of apoptotic cells *in vitro* by TUNEL and fluorescent activated cell sorting (FACS)**

Human umbilical vein endothelial cells (HUVEC) were maintained in Endothelial Cell Growth Medium (PromoCell, Heidelberg, Germany) and grown to 80% confluence, trypsinized and preincubated for 20 minutes in serum-free medium alone or medium containing 100 nM, 500 nM, 1  $\mu$ M, 10  $\mu$ M, 25  $\mu$ M, or 50  $\mu$ M JSM 6427 or 10  $\mu$ M camptothecin. Cells ( $4 \times 10^5$ ) were plated in 6-well plates coated with 10  $\mu$ g/ml fibronectin (Chemicon Europe, Hampshire, United Kingdom) and grown for 48 hours. Adherent and non-adherent cells were collected, pooled and washed. Cells were fixed in 1% paraformaldehyde for 30 minutes on ice, washed and carefully resuspended in 70% cold ethanol. TUNEL was performed using the APO-Direct kit (BD Pharmingen, San Diego, CA). Briefly, cells were incubated with TdT enzyme and FITC-dUTP in reaction buffer for 60 minutes (positive and negative cells of the kit) or 180 minutes (probes) at 37°C. Cells were rinsed and incubated with PI-staining solution for 30 minutes to determine total cell numbers. FACS analysis was performed using a FACS-Calibur (BD Bioscience, San Diego, CA) and the CellQuest software.

### **Western Blotting**

ARPE19 cells were incubated in serum-free DMEM/Ham's F12 (Biochrom AG, Berlin, Germany) culture medium for 16 hours. Plates were coated with 10  $\mu$ g/ml fibronectin or 0.002 % poly-L-lysine (Sigma-Aldrich, Munich, Germany) and blocked with 1% BSA. Cells were trypsinized and held in suspension for 30 minutes. Subsequently,  $1 \times 10^6$  cells were incubated with compounds for 10 minutes. Cells were allowed to adhere for 15 minutes on fibronectin in serum-

free medium. Adherent cells and cells from supernatants were lysed in 150  $\mu$ l lysis buffer (1% NP40, 150mM NaCl, 50mM Tris-HCl, pH 7.5, protease-inhibitor-cocktail (Sigma-Aldrich), 25 mM glycerolphosphate, 50 mM NaF, 10 mM  $\text{Na}_4\text{P}_2\text{O}_7$ , 1 mM orthovanadate) on ice. Lysates were centrifuged and equal amounts of protein were separated on a 4-15% Tris/HCl gel by SDS-PAGE and transferred to PVDF membranes by semi-dry Western Blotting. Membranes were blocked in 3% BSA. Phosphorylated extracellular signal regulated kinase (ERK) and total ERK were detected with a phospho-specific ERK1/2 (pT202/pY204) antibody (Cell Signaling, Danvers, MA) and a p44/42 MAP kinase antibody (Cell Signaling). Bands were visualized with POD conjugated anti-rabbit and anti-mouse antibodies (Sigma-Aldrich) and BM Chemiluminescence Western Blotting POD-substrate (Roche Applied Science, Mannheim, Germany). The luminescence signal was measured and quantified using a Lumi imager (Boehringer Mannheim, Mannheim, Germany) and corresponding software.

## Results

### **Expression of integrin $\alpha_5$ subunit is increased in vascular cells participating in choroidal neovascularization**

Two weeks after laser-induced rupture of Bruch's membrane staining with GSA showed large choroidal neovascularization lesions at rupture sites (Figure 1A, arrows). Adjacent sections immunohistochemically stained for integrin  $\alpha_5$  subunit showed strong labeling throughout the entire choroidal neovascularization lesion (Figure 1B, arrows). Superimposed images from DAPI stained sections showed the overlying neural retina confirming that the cells labeled with anti- $\alpha_5$  are in the subretinal space (Figure 1C). Regions of retina remote from Bruch's membrane rupture sites showed no choroidal neovascularization and no staining for  $\alpha_5$  subunit (Figure 1D-F). This suggests that expression of  $\alpha_5$  subunit in vascular cells in the eye under normal circumstances is below the sensitivity of our staining technique to detect it, but there is strong upregulation of  $\alpha_5$  subunit expression in vascular cells participating in choroidal neovascularization.

### **JSM6427 is a selective antagonist of integrin $\alpha_5\beta_1$**

The integrin inhibitor JSM6427 is an antagonist of binding to integrin  $\alpha_5\beta_1$  and is at least 1200-fold less potent in the inhibition of binding to  $\alpha_v\beta_3$ , the integrin that is most closely related to  $\alpha_5\beta_1$  in structure (Table 1). The selectivity

against other integrins such as  $\alpha_V\beta_5$  and  $\alpha_{IIb}\beta_3$  is significantly higher, 3,700-fold or > 100,000-fold, respectively (data not shown).

### **Subcutaneous delivery of JSM6427 suppresses choroidal neovascularization**

Osmotic minipumps (Figure 2A) that release 1.5 or 10  $\mu\text{g}$  per hour of JSM6427 or vehicle alone were implanted beneath the skin on the backs of mice (Figure 2B) and the following day Bruch's membrane was ruptured in 3 locations in each eye. Fourteen days after rupture of Bruch's membrane, the size of choroidal neovascularization lesions at rupture sites in mice that received 1.5 or 10  $\mu\text{g}$  per hour of JSM6427 (Figure 2C and F) appeared smaller than corresponding controls that received infusion of vehicle (Figure 2D and G). Measurement of the size of the lesions by image analysis confirmed that for both infusion rates of JSM6427, 1.5 (Figure 2E) and 10  $\mu\text{g}$  per hour (Figure 2H), choroidal neovascularization lesions were significantly smaller than corresponding vehicle controls by about 33% or 40%, respectively.

### **Subcutaneous delivery of JSM6427 causes regression of established choroidal neovascularization**

Mice had laser-induced rupture of Bruch's membrane and after 7 days some mice were used to measure the baseline amount of choroidal neovascularization (Figure 3A). The remainder of the mice had implantation of an osmotic minipump that released 10  $\mu\text{g}/\text{hour}$  of JSM6427 or vehicle. After 7



days of treatment, the mice infused with JSM6427 had small choroidal neovascularization lesions at Bruch's membrane rupture sites (Figure 3B), while mice infused with vehicle had lesions that appeared larger (Figure 3C). TUNEL showed labeling within the outer nuclear layer (ONL) of the retina overlying choroidal neovascularization in day 7 baseline eyes (Figure 3D). This is likely to be a consequence of the laser photocoagulation that was used to induce rupture of Bruch's membrane, although it is possible that the presence of choroidal neovascularization is damaging to the overlying retina due to interference with transmission of oxygen from the choroid, interference with transmission of survival signals from the retinal pigmented epithelium, or some other reason. At 14 days after rupture of Bruch's membrane, mice infused with JSM6427 for the previous 7 days (Figure 3E) and those infused with vehicle (Figure 3F) showed apoptosis in the retina overlying choroidal neovascularization, but only the mice infused with JSM6427 showed apoptosis of vascular cells within the choroidal neovascularization as expected for the proposed mechanism of action and confirmed with *in vitro* apoptosis assays (see below, Figure 4). Figure 3G shows the boxed region in Figure 3E at high magnification providing better visualization of 2 yellow cells (arrows) due to colocalization of GSA and ApopTag red. Measurement of the size of choroidal neovascularization lesions by image analysis showed that mice infused with JSM6427 had significantly smaller lesions than those seen at baseline or those seen in mice infused with vehicle (Figure 3H). This indicates that continuous systemic infusion of JSM6427 causes regression of choroidal neovascularization.

### **JSM6427 causes apoptosis of vascular endothelial cells *in vitro***

HUVEC cells were grown in fibronectin-coated wells for 48 hours in serum-free medium containing various concentrations of JSM6427. Camptothecin, a strong inducer of apoptosis, was used as a positive control. JSM6427 caused a dose-dependent increase in the percentage of TUNEL-positive cells in cultures ranging from 44% for those incubated with 50  $\mu$ M to 6% for those incubated in 100 nM (Figure 4). In cultures incubated in serum-free medium, 5% of cells were TUNEL-positive and 82% of cells were labelled in cultures incubated with 10  $\mu$ M camptothecin. These data show that JSM6427 induces apoptosis of vascular endothelial cells.

### **JSM6427 reduces fibronectin-induced phosphorylation of ERK**

The mechanism by which ECM components generate survival signals through integrins involves increased phosphorylation of intracellular messengers that increase expression of apoptosis inhibitors such as Bcl-2 (Lee and Ruoslahti, 2005). Phosphorylation of ERK plays a central role in fibronectin-mediated survival signaling through  $\alpha_5\beta_1$  in brain capillary endothelial cells (Wang and Milner, 2006). Therefore, we investigated the effect of JSM6427 on fibronectin-induced phosphorylation of ERK in ARPE19 cells, which express  $\alpha_5\beta_1$ . Serum starved ARPE19 cells were preincubated with JSM6427 for 10 min in suspension and plated for 15 min on fibronectin, poly-L-lysine, or kept in suspension. Western blots showed that for cells not pre-incubated in JSM6427, those plated on fibronectin had a much stronger signal for phosphorylated ERK

than those plated on poly-L-lysine or those kept in suspension (Figure 5A). Pre-incubation with JSM6427 prior to plating on fibronectin caused a dose-dependent reduction in the amount of phosphorylated ERK in the cultures. Quantification of the signal for phosphorylated ERK normalized to the total amount of ERK showed that pre-incubation with 10  $\mu$ M JSM6427 completely eliminated the fibronectin-induced stimulation of ERK phosphorylation (Figure 5B) and the  $IC_{50}$  was 0.23  $\mu$ M (Figure 5C).

### **Two intravitreal injections of JSM6427 did not cause significant suppression of choroidal neovascularization**

To explore the feasibility of local delivery of JSM6427, mice had laser-induced rupture of Bruch's membrane followed by intravitreal injection of vehicle or vehicle containing 3 or 20  $\mu$ g of JSM6427 immediately after laser and 7 days later. Fourteen days after laser the area of choroidal neovascularization was measured by image analysis. The size of choroidal neovascularization lesions appeared somewhat smaller in eyes treated with JSM6427, but there was not a statistically significant difference compared to vehicle-treated or untreated eyes (Figure 6). This suggests that weekly intravitreal injections in mice are not able to maintain levels of JSM6427 sufficient to significantly inhibit choroidal neovascularization.

## Discussion

In this study, we have shown that  $\alpha_5\beta_1$  integrin is strongly upregulated in choroidal neovascularization. This marked differential in expression between vascular cells participating in choroidal neovascularization and vascular cells in established choroidal vessels, suggests that  $\alpha_5\beta_1$  may play an important role in growth and maintenance of the new vessels and blocking  $\alpha_5\beta_1$  may provide a way to selectively target choroidal neovascularization. Using a selective antagonist of  $\alpha_5\beta_1$ , JSM6427, we found this to be the case. Sustained systemic delivery of JSM6427 using an osmotic minipump suppressed the development of choroidal neovascularization and when infusion was started after the neovascularization was established, it caused it to regress. TUNEL staining showed selective apoptosis in vascular cells participating in the neovascularization in JSM6427-treated mice. This suggests that signaling through  $\alpha_5\beta_1$  provides a critical survival signal to endothelial cells in choroidal new vessels that when blocked triggers apoptosis. Endothelial cells in established vessels must develop alternative survival signal pathways that eliminate the dependence on  $\alpha_5\beta_1$  signaling manifested by endothelial cells in choroidal neovascular lesions. Such a switch has been noted when cerebral vessels mature and change from an angiogenic to a mature phenotype; they stop expressing  $\alpha_5\beta_1$  and  $\alpha_4\beta_1$ , and begin to express  $\alpha_1\beta_1$  and  $\alpha_6\beta_1$ . (Milner,2002)

The exquisite selectivity for JSM6427-induced apoptosis for endothelial cells in

choroidal neovascularization compared to mature choroidal vessels predicts a good safety profile.

Cell signaling through which integrins promote cells survival is complex (for review see (Giancotti and Ruoslahti, 1999)). Binding of most integrins to a ligand in the ECM activates focal adhesion kinase (FAK), which plays a role in most integrin-mediated effects; survival signaling occurs by activation of FAK along with other signaling molecules that act together to increase levels of Bcl-2 or other inhibitors of apoptosis (Lee and Ruoslahti, 2005). Phosphorylation of ERK plays a central role in stimulation of brain capillary endothelial cell survival by fibronectin through  $\alpha_5\beta_1$  (Wang and Milner, 2006). JSM6427 blocks fibronectin-induced phosphorylation of ERK, which likely plays a role in its induction of apoptosis.

Despite the apparent safety of sustained systemic administration of JSM6427, local administration has the theoretical benefit of limiting exposure to the rest of the body and reducing the total amount of JSM6427 that is required for treatment. Two intravitreal injections of JSM6427 over the course of 2 weeks failed to suppress choroidal neovascularization. A possible explanation is that sustained exposure of JSM6427 to endothelial cells in choroidal neovascular lesions is necessary to perturb survival signals and even brief lapses in blockade of  $\alpha_5\beta_1$  signaling may be sufficient to prevent apoptosis. In the future, it will be worthwhile to test this hypothesis by assessing the effect of sustained local delivery of JSM6427.

Choroidal neovascularization occurs in diseases of the retinal pigmented epithelium/Bruch's membrane complex. The most common of these is age-related macular degeneration (AMD), which is the most prevalent cause of severe vision loss in patients over the age of 60 in developed countries (Klein et al., 1993). Studies in animal models have demonstrated that VEGF is an important stimulus and that VEGF antagonists suppress the neovascularization (Kryzstolik et al., 2002; Kwak et al., 2000; Saishin et al., 2003). The role of VEGF in patients with neovascular AMD has now been confirmed in a clinical trial demonstrating that multiple intravitreal injections of pegaptanib, an aptamer that binds VEGF, slows the rate of visual loss (Gragoudas et al., 2004). This is a useful start to pharmacotherapy for choroidal neovascularization, but further improvements are needed. Regression of choroidal neovascularization is not achieved in patients treated with pegaptanib; the size of lesions continued to increase over the course of a year, although at a slower rate than that seen in patients that did not receive pegaptanib. Antagonism of VEGF appears to reduce excessive permeability and slows growth, but does not cause involution of choroidal neovascularization. VEGF provides some survival signals to newly developed endothelial cells (Alon et al., 1995), but survival signals from the extracellular matrix may be sufficient to allow continued growth of choroidal neovascular lesions, although at a slower rate. Combination treatment using JSM6427 with a VEGF antagonist may be extremely useful since perturbation of at least one source of matrix-derived survival signaling along with elimination of

the survival signal provided by VEGF may be an effective means to promote involution of choroidal neovascularization.

## Acknowledgement

The authors thank Sascha Birkner for her assistance with some of the *in vitro* experiments.



## References

- Alon T, Hemo I, Itin A, Pe'er J, Stone J and Keshet E. 1995. Vascular endothelial growth factor acts as a survival factor for newly formed retinal vessels and has implications for retinopathy of prematurity. *Nature Med* 1:1024-1028.
- Bardos JI, Chau NM and Ashcroft M. 2004. Growth factor mediated induction of HDM2 positively regulates hypoxia-inducible factor 1alpha expression. *Mol Cell Biol* 24:2905-2914.
- Brooks P, Clark R and Cheresh D. 1994a. Requirement of vascular integrin alpha-v beta-3 for angiogenesis. *Science* 264:569-571.
- Brooks PC, Montgomery AM, Rosenfeld M, Reisfeld RA, Hu T, Klier G and Cheresh D. 1994b. Integrin alpha v beta 3 antagonists promote tumor regression by inducing apoptosis of angiogenic blood vessels. *Cell* 79:1157-1164.
- Collo G and Pepper MS. 1999. Endothelial cell integrin alpha5beta1 expression is modulated by cytokines and during migration *in vitro*. *J Cell Sci* 112:569-578.
- Giancotti FG and Ruoslahti E. 1999. Integrin signaling. *Science* 285:1028-1032.
- Gragoudas ES, Adamis AP, Cunningham ET, Jr., Feinsod M and Guyer DR. 2004. Pegaptanib for neovascular age-related macular degeneration. *N Eng J Med* 351:2805-2816.
- Haddad JJ and Harb HL. 2005. Cytokines and the regulation of hypoxia-inducible factor (HIF)-1alpha. *Int Immunopharmacol* 5:461-483.

Hammes H, Brownlee M, Jonczyk A, Sutter A and Preissner K. 1996.

Subcutaneous injection of a cyclic peptide antagonist of vitronectin receptor-type integrins inhibits retinal neovascularization. *Nat Med* 2:529-533.

Hynes RO. 2002. A reevaluation of integrins as regulators of angiogenesis. *Nat Med* 8:918-921.

Kim S, Bell K, Mousa SA and Varner JA. 2000. Regulation of angiogenesis in vivo by ligation of integrin alpha5beta1 with the central cell-binding domain of fibronectin. *Am J Pathol* 156:1345-1362.

Klein R, Klein BEK and Linton KP. 1993. The Beaver Dam Eye Study: the relation of age-related maculopathy to smoking. *Am J Epidemiol* 137:190-200.

Kryzstolik MG, Afshari MA, Adamis AP, Gaudreault J, Gragoudas ES, Michaud NM, Li W, Connolly E, O'Neill CA and Miller JW. 2002. Prevention of experimental choroidal neovascularization with intravitreal anti-vascular endothelial growth factor antibody fragment. *Arch Ophthalmol* 120:338-346.

Kwak N, Okamoto N, Wood JM and Campochiaro PA. 2000. VEGF is an important stimulator in a model of choroidal neovascularization. *Invest Ophthalmol Vis Sci* 41:3158-3164.

Lee B-H and Ruoslahti E. 2005. Alpha5beta1 integrin stimulates Bcl-2 expression and cell survival through Akt, focal adhesion kinase, and Ca<sup>2+</sup>/calmodulin-dependent protein kinase IV. *J Cell Biochem* 95:1214-1223.

- Luna J, Tobe T, Mousa SA, Reilly TM and Campochiaro PA. 1996. Antagonists of integrin alpha-v beta-3 inhibit retinal neovascularization in a murine model. *Lab Invest* 75:563-573.
- Magnussen A, Kasman IM, Norberg S, Baluk P, Murray R and McDonald DM. 2005. Rapid access of antibodies to alpha5beta1 integrin overexpressed on the luminal surface of tumor blood vessels. *Cancer Res* 65:2712-2721.
- Manalo DJ, Rowan A, Lavoie T, Natarajan L, Kelly BD, Ye SQ, Garcia JG and Semenza GL. 2005. Transcriptional regulation of vascular endothelial cell responses to hypoxia by HIF-1. *Blood* 105:659-669.
- Milner R and Campbell IL. 2002. Developmental regulation of beta1 integrins during angiogenesis in the central nervous system. *Mol Cell Neurosci* 20:616-626.
- Ozaki H, Okamoto N, Ortega S, Chang M, Ozaki K, Sadda S, Viores MA, Derevjanik N, Zack DJ, Basilico C and Campochiaro PA. 1998. Basic fibroblast growth factor is neither necessary nor sufficient for the development of retinal neovascularization. *Am J Pathol* 153:757-765.
- Parsons-Wingenter P, Kasman IM, Norberg S, Magnussen A, Zanivan S, Rissone A, Baluk P, Favre CJ, Jeffry U, Murray R and McDonald DM. 2005. Uniform overexpression and rapid accessibility of alpha5beta1 integrin on blood vessels in tumors. *Am J Pathol* 167:193-211.
- Ribatti D. 2005. The crucial role of vascular permeability factor/vascular endothelial growth factor in angiogenesis: a historical review. *Br J Haematol* 128:303-309.

Saishin Y, Saishin Y, Takahashi K, Lima Silva R, Hylton D, Rudge J, J. WS and

Campochiaro PA. 2003. VEGF-TRAP<sub>R1R2</sub> suppresses choroidal neovascularization and VEGF-induced breakdown of the blood-retinal barrier. *J Cell Physiol* 195:241-248.

Sottile J. 2004. Regulation of angiogenesis by extracellular matrix. *Biochim Biophys Acta* 1654:13-22.

Stoeltzing O, Liu W, Reinmuth NF, F., Parry GC, Parikh AA, McCarty MF, Bucana CD, Mazar AP and Ellis LM. 2003. Inhibition of integrin alpha5beta1 function with a small peptide (ATN-161) plus continuous 5-FU infusion reduces colorectal liver metastases and improves survival in mice. *Int J Cancer* 104:496-503.

Tobe T, Ortega S, Luna JD, Ozaki H, Okamoto N, Derevjani NL, Viores SA, Basilico C and Campochiaro PA. 1998. Targeted disruption of the *FGF2* gene does not prevent choroidal neovascularization in a murine model. *Am J Pathol* 153:1641-1646.

Wang J and Milner R. 2006. Fibronectin promotes brain capillary endothelial cell survival and proliferation through alpha<sub>5</sub>beta<sub>1</sub> and alpha<sub>v</sub>beta<sub>3</sub> integrins via MAP kinase signalling. *J Neurochem* 96:148-159.

Yang JT, Rayburn H and Hynes RO. 1993. Embryonic mesodermal defects in alpha5 integrin-deficient mice. *Development* 119:229-238.

## Figure Legends

### **Figure 1. Immunohistochemical staining for integrin $\alpha_5$ subunit in mice with choroidal neovascularization.**

Adult C57BL/6J mice had laser-induced rupture of Bruch's membrane in each eye. Two weeks after laser treatment, mice were euthanized, eyes were removed, and frozen sections were cut through rupture sites. Some sections were stained with which selectively stains vascular cells and allows visualization of choroidal neovascularization (A). Adjacent sections were immunohistochemically stained for integrin  $\alpha_5$  subunit (B). Superimposed image from a DAPI-stained section shows the retinal cells in the outer nuclear layer (ONL), inner nuclear layer (INL), and ganglion cell layer (GCL) confirming that the cells expressing  $\alpha_5$  integrin are in the subretinal space (C). Retina and choroid remote from Bruch's membrane rupture sites showed staining of retinal vessels with GSA, but no choroidal neovascularization (D) and no staining for integrin  $\alpha_5$  subunit (E and F).

Bar = 100  $\mu$ m

### **Figure 2. Systemic delivery of JSM6427 by osmotic minipump suppresses the development of choroidal neovascularization at Bruch's membrane rupture sites.**

A. The osmotic minipumps were about 30 mm in length.

B. The implanted minipumps were visible as humps (arrows) beneath the skin of the back.

Mice implanted with pumps containing 3 mg/ml of JSM6427 received about 1.5  $\mu\text{g}/\text{hour}$  of JSM6427 and choroidal flat mounts after perfusion with fluorescein-labeled dextran showed small areas of choroidal neovascularization at rupture sites (C, arrows) compared to areas of choroidal neovascularization seen in mice implanted with pumps containing vehicle (D, arrows). Image analysis confirmed that there was significantly less choroidal neovascularization in mice that received 1.5  $\mu\text{g}/\text{hour}$  of JSM6427 compared to those that received vehicle (E). Mice implanted with pumps containing 20 mg/ml of JSM6427 received about 10  $\mu\text{g}/\text{hour}$  of JSM6427 and also appeared to have smaller areas of choroidal neovascularization (F, arrows) than mice that received vehicle (G, arrows). Image analysis showed a statistically significant difference from vehicle (H) in the same range as that seen after infusion of 1.5  $\mu\text{g}/\text{hour}$  of JSM6427.

\* $p = 0.0005$ , † $p = 6 \times 10^{-8}$  by Mann-Whitney U test

Bar = 100  $\mu\text{m}$

**Figure 3. Systemic delivery of JSM6427 by osmotic minipump causes regression of choroidal neovascularization.**

Adult C57BL/6J mice had laser-induced rupture of Bruch's membrane at 3 locations in each eye. Seven days after laser treatment, 9 mice were perfused with fluorescein-labeled dextran and the baseline amount of choroidal neovascularization at 7 days (A, arrows) was measured by image analysis. The

remainder of the mice had implantation of an osmotic minipump containing 20 mg/ml of JSM6427 (B) or vehicle (C), and these mice were perfused with fluorescein-labeled dextran on day 14. In mice that received JSM6427, the area of choroidal neovascularization lesions (B, arrows) appeared smaller than those in mice treated with vehicle (C, arrows) and the baseline amount seen at day 7 (A, arrows). TUNEL (red) of sections also stained with *Griffonia simplicifolia* lectin (GSA), which stains vascular cells (green), and DAPI, which stains cell nuclei (blue) showed apoptotic cells in the outer nuclear layer (ONL) in day 7 baseline eyes (D), a consequence of the laser treatment 7 days before. Sections from day 14 eyes that had been treated with JSM6427 also showed apoptotic cells in the ONL, but in addition there were yellow cells within choroidal neovascularization lesions (E and G, arrows) due to colocalization of TUNEL and GSA, indicating apoptosis of cells with the choroidal neovascularization. Sections from eye treated with vehicle showed apoptotic cells in the ONL, but not within the choroidal neovascularization (F). Measurement of the area of choroidal neovascularization by image analysis confirmed that there was a significant reduction in mice treated with JSM6427 compared to the amount seen at baseline or in mice treated with vehicle (H).

\* $p = 0.0039$  by linear mixed model for comparison with baseline; † $p = 0.0283$  by linear mixed model for comparison with vehicle. P values were adjusted for multiple comparisons using Dunnett's method.

A-F, bar = 100  $\mu\text{m}$ ; G, bar = 50  $\mu\text{m}$

**Figure 4. JSM6427 induces apoptosis in cultured vascular endothelial cells.**

Human umbilical vein endothelial cells were grown in fibronectin coated dishes for 48 hours in serum-free medium containing various concentrations of JSM6427 or camptotecin. TUNEL-stained cells were detected by fluorescent activated cell sorting. Each bar shows the mean ( $\pm$ SD) % of apoptotic cells per culture generated from one experiment performed in triplicate.

\*  $p < 0.01$  by ANOVA with Dunnett's correction for multiple comparisons.

**Figure 5. JSM6427 reduces fibronectin-induced phosphorylation of ERK.**

Serum starved ARPE19 cells were preincubated in suspension for 10 minutes with serum-free medium or medium containing various concentrations of JSM6427. The cells were then kept in suspension (susp) or plated on fibronectin (FN) or poly-L-lysine (PL). After 15 minutes cells were lysed and the lysates were run in Western blots using an antibody directed against phosphorylated ERK or ERK.

A. Western blots showed that for cells not pre-incubated in JSM6427, those plated on FN had a much stronger signal for phosphorylated ERK than those plated on poly-L-lysine or those kept in suspension. Pre-incubation with JSM6427 prior to plating on FN caused a dose-dependent reduction in the amount of phosphorylated ERK in the cultures.

B. Band intensity on Western blots was quantified using a Lumi Imager. The amount of phosphorylated ERK was normalized to the total amount of ERK and



the phosphorylation of cells plated on fibronectin was set at 100%. This quantification confirmed that JSM6427 reduced fibronectin-induced phosphorylation of ERK. Pre-incubation with 10  $\mu$ M JSM6427 completely eliminated the fibronectin-induced stimulation of ERK phosphorylation.

C. The IC<sub>50</sub> value was calculated using XLFit software. All of these results were replicated in an independent experiment.

**Figure 6. Two intravitreal injections of JSM6427 failed to suppress choroidal neovascularization at Bruch's membrane rupture sites.**

Adult C57BL/6J mice had rupture of Bruch's membrane at 3 locations in each eye. On days 0 and 7 after laser treatment, mice were given an intravitreal injection of 3 or 20  $\mu\text{g}$  of JSM6427 in one eye and vehicle in the fellow eye. At day 14, mice were perfused with fluorescein-labeled dextran and the area of choroidal neovascularization at Bruch's membrane rupture sites was measured by image analysis. There was no statistically significant difference in the size of choroidal neovascularization lesions in eyes injected with 3  $\mu\text{g}$  (A) or 20  $\mu\text{g}$  of JSM6427 (B) compared to either fellow eyes treated with vehicle or uninjected eyes.

**Figure 1**

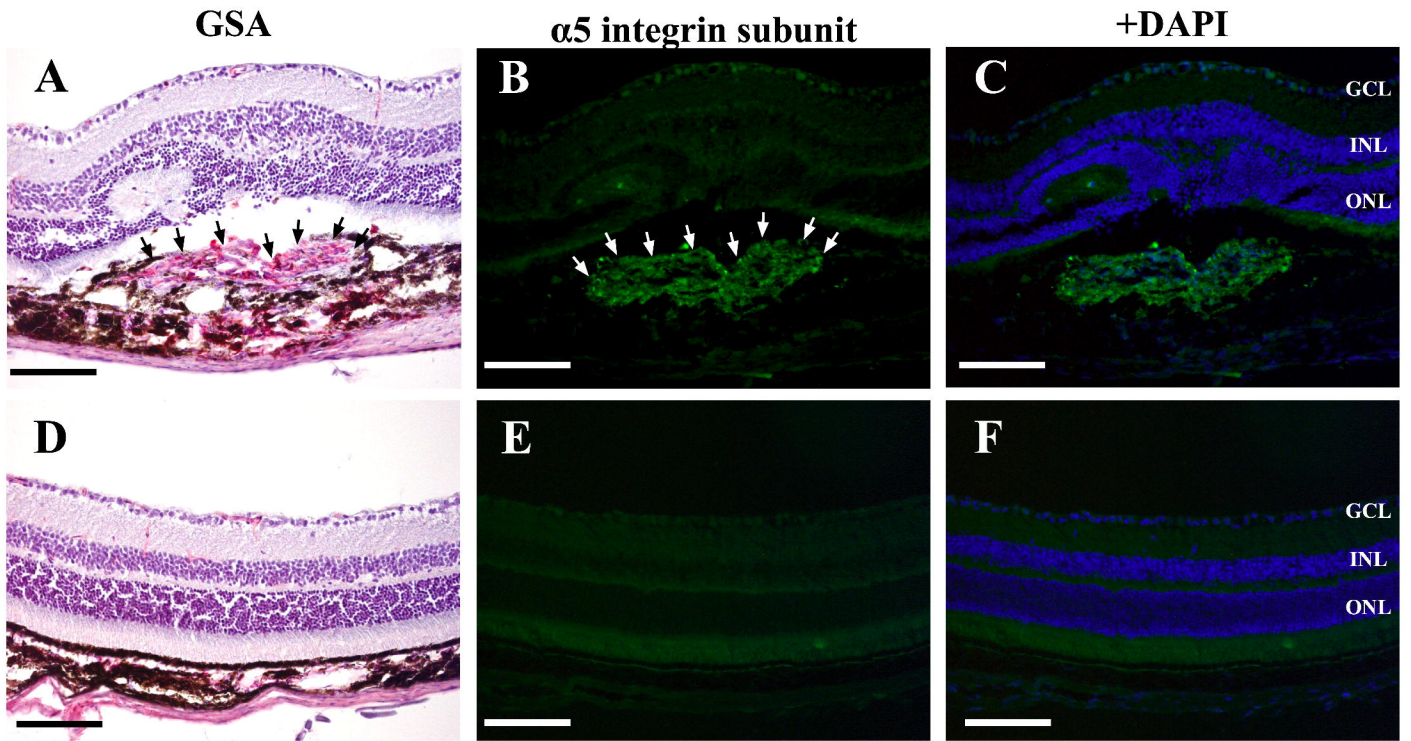
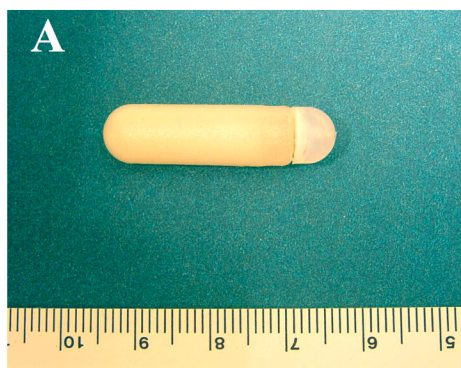
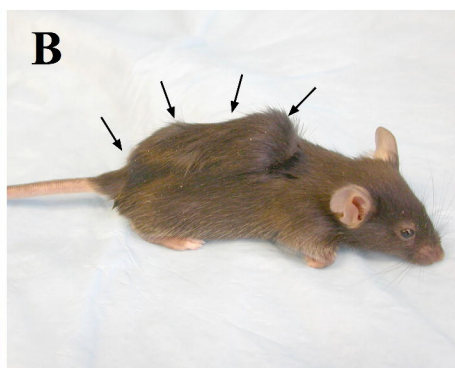


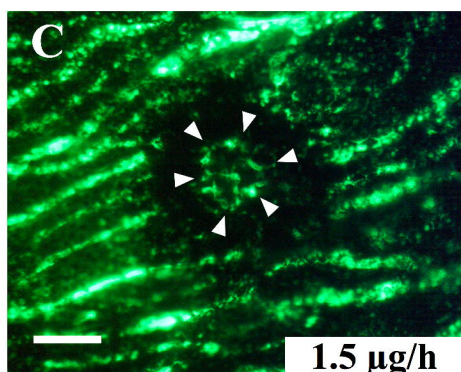
**Figure 2**



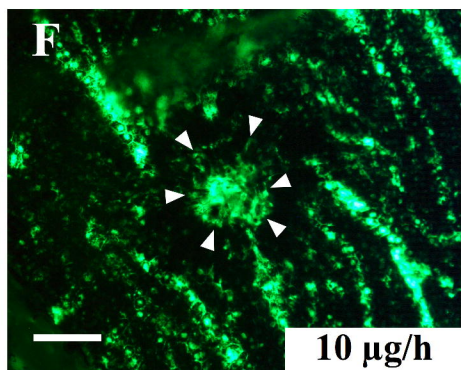
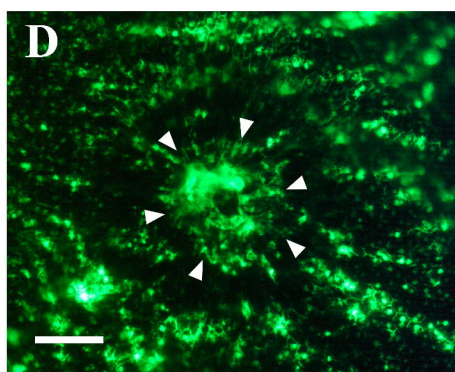
**JSM6427**



**Vehicle**



**1.5  $\mu\text{g/h}$**



**10  $\mu\text{g/h}$**

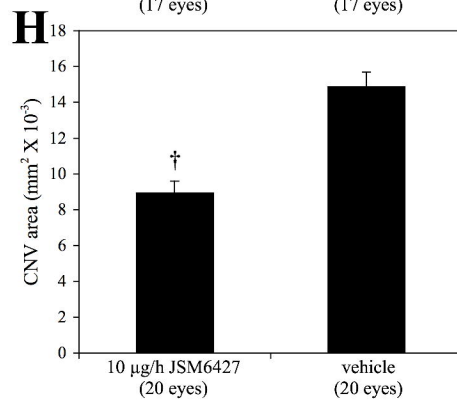
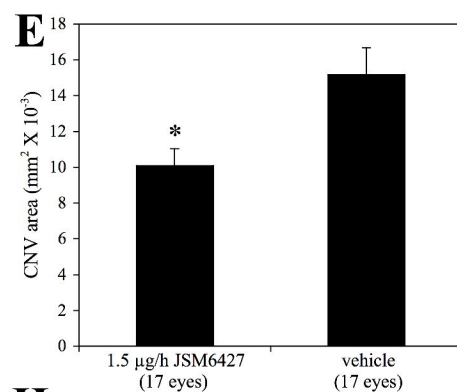
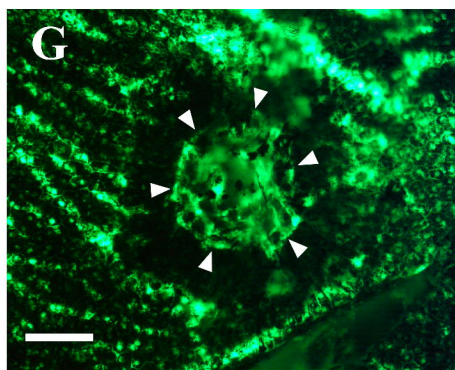


**Figure 3**

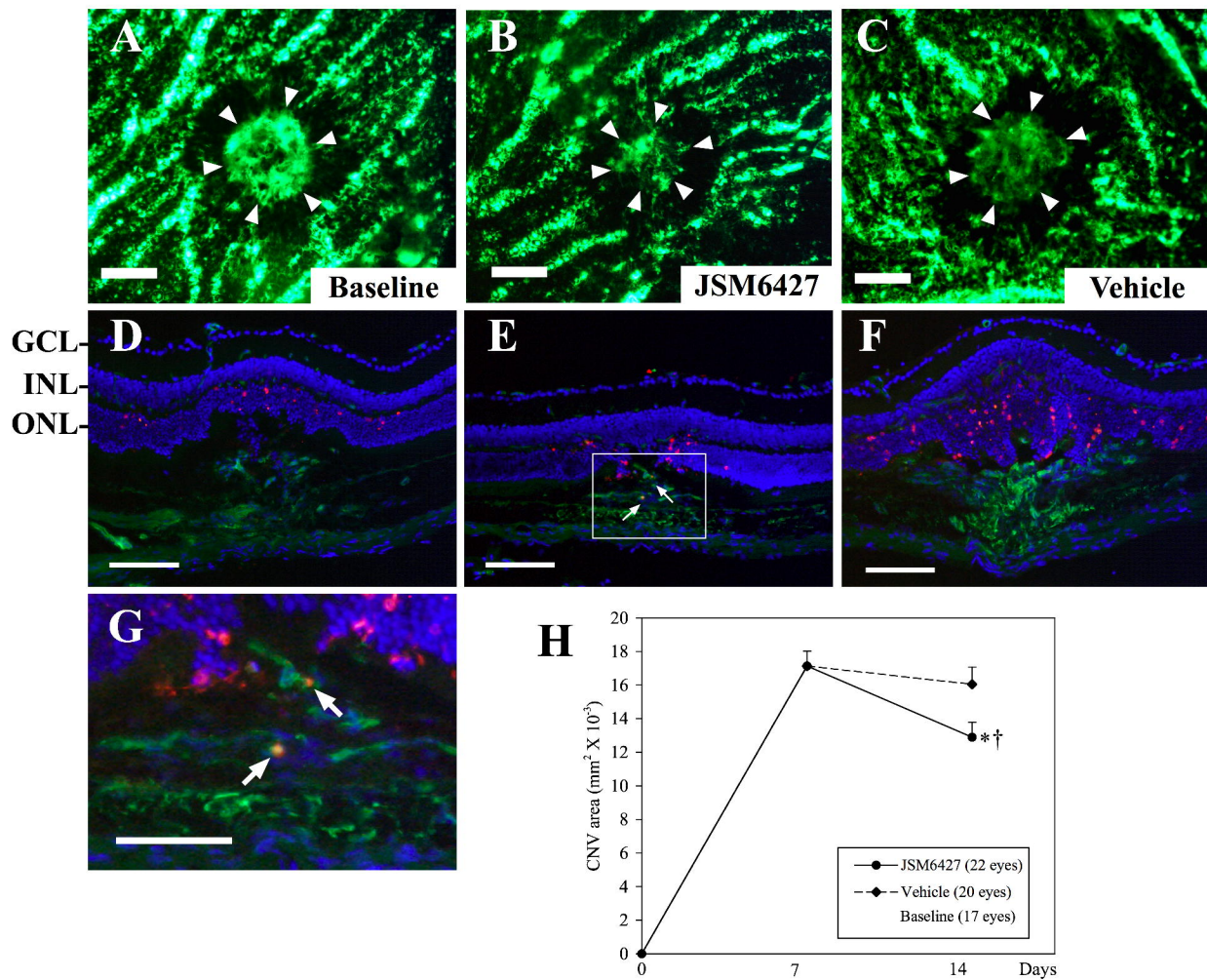


Figure 4

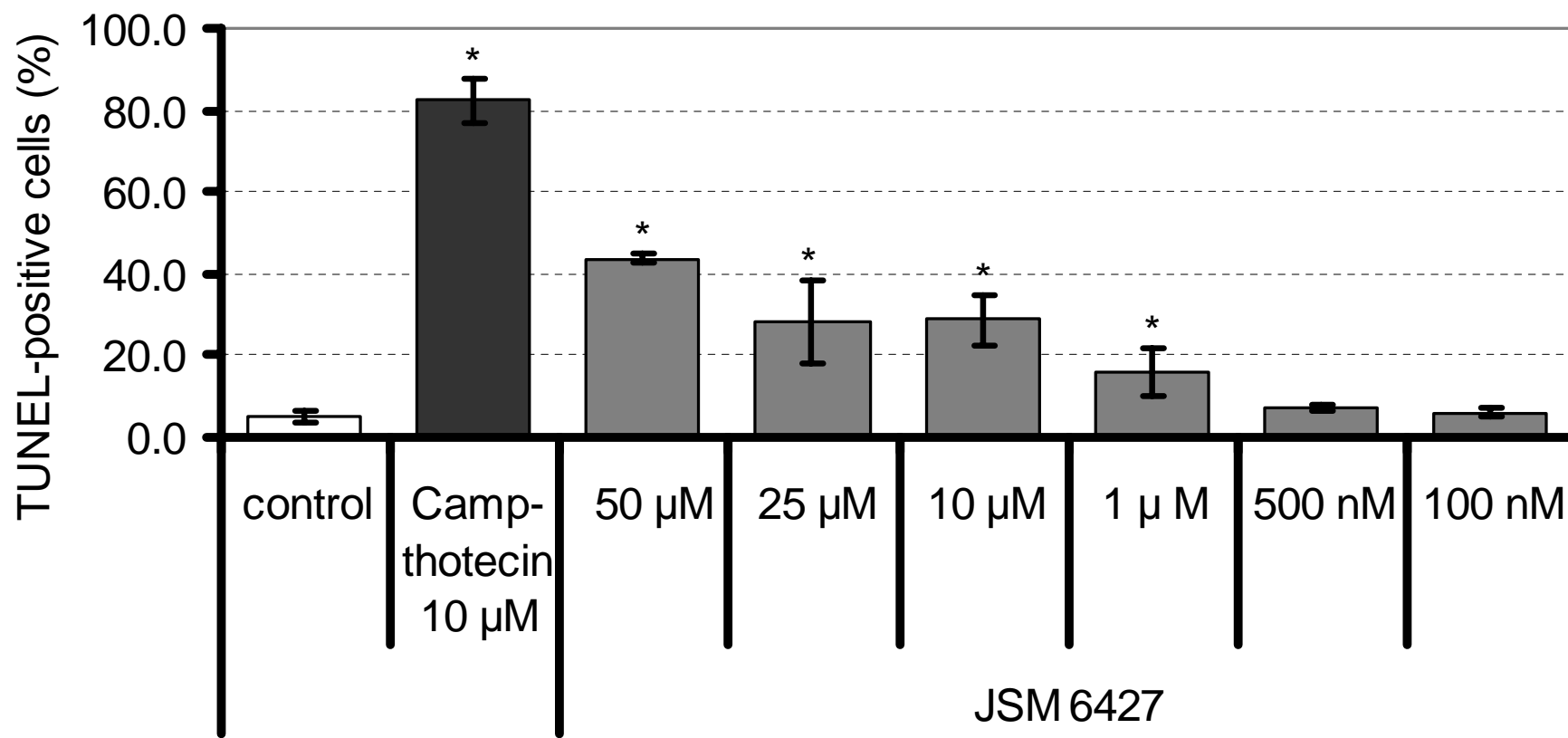
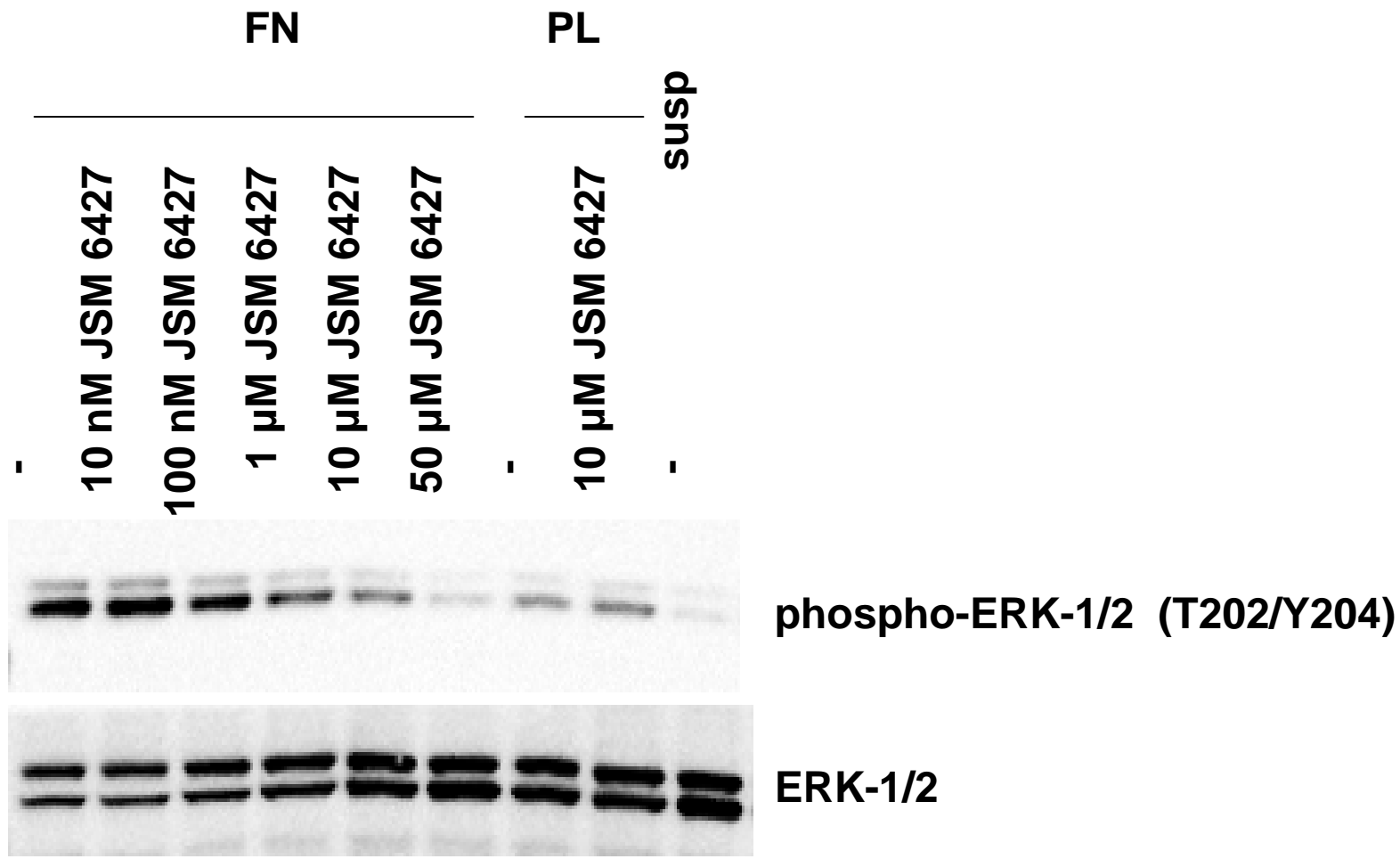


Figure 5A



**Figure 5B**

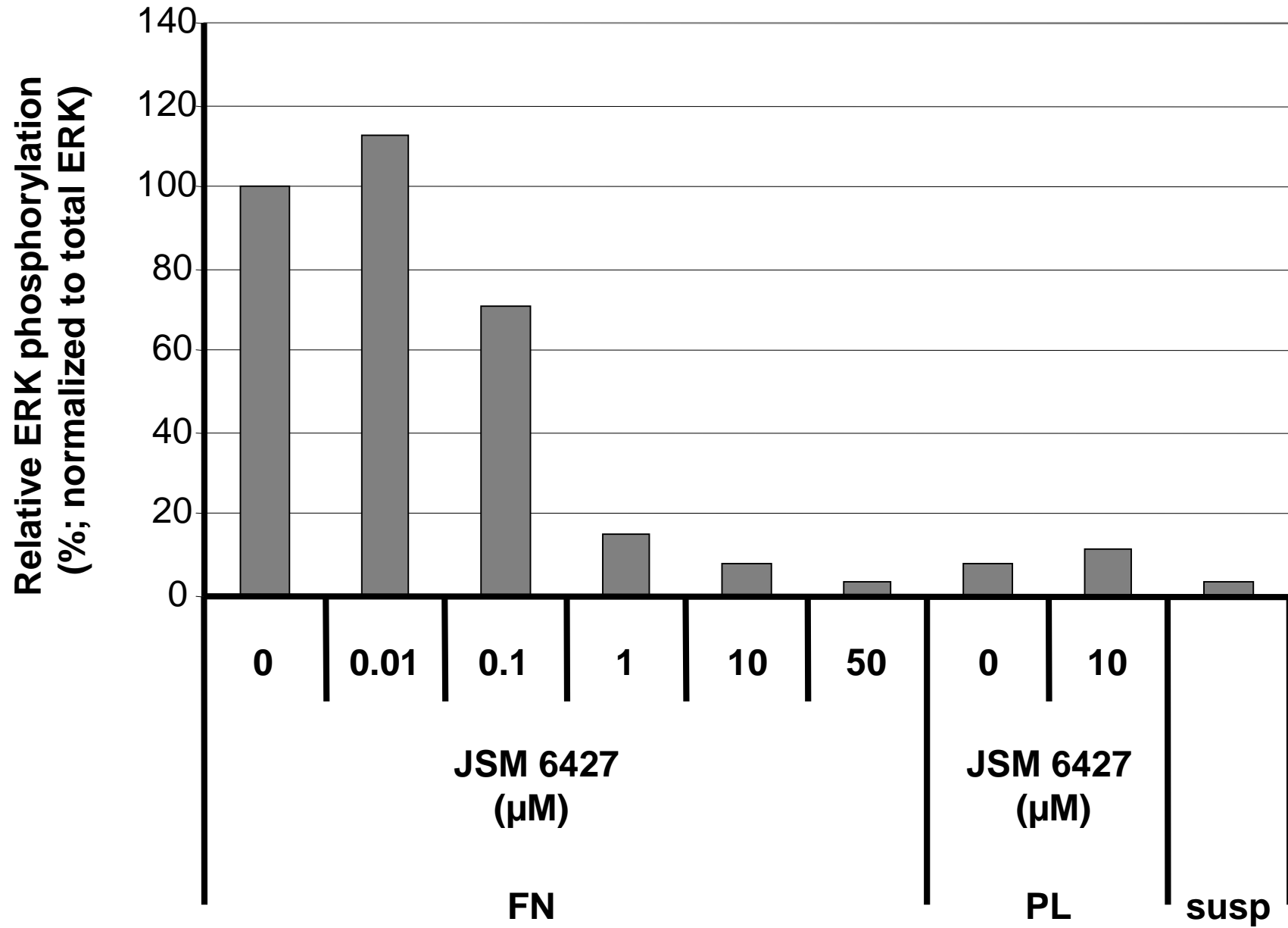
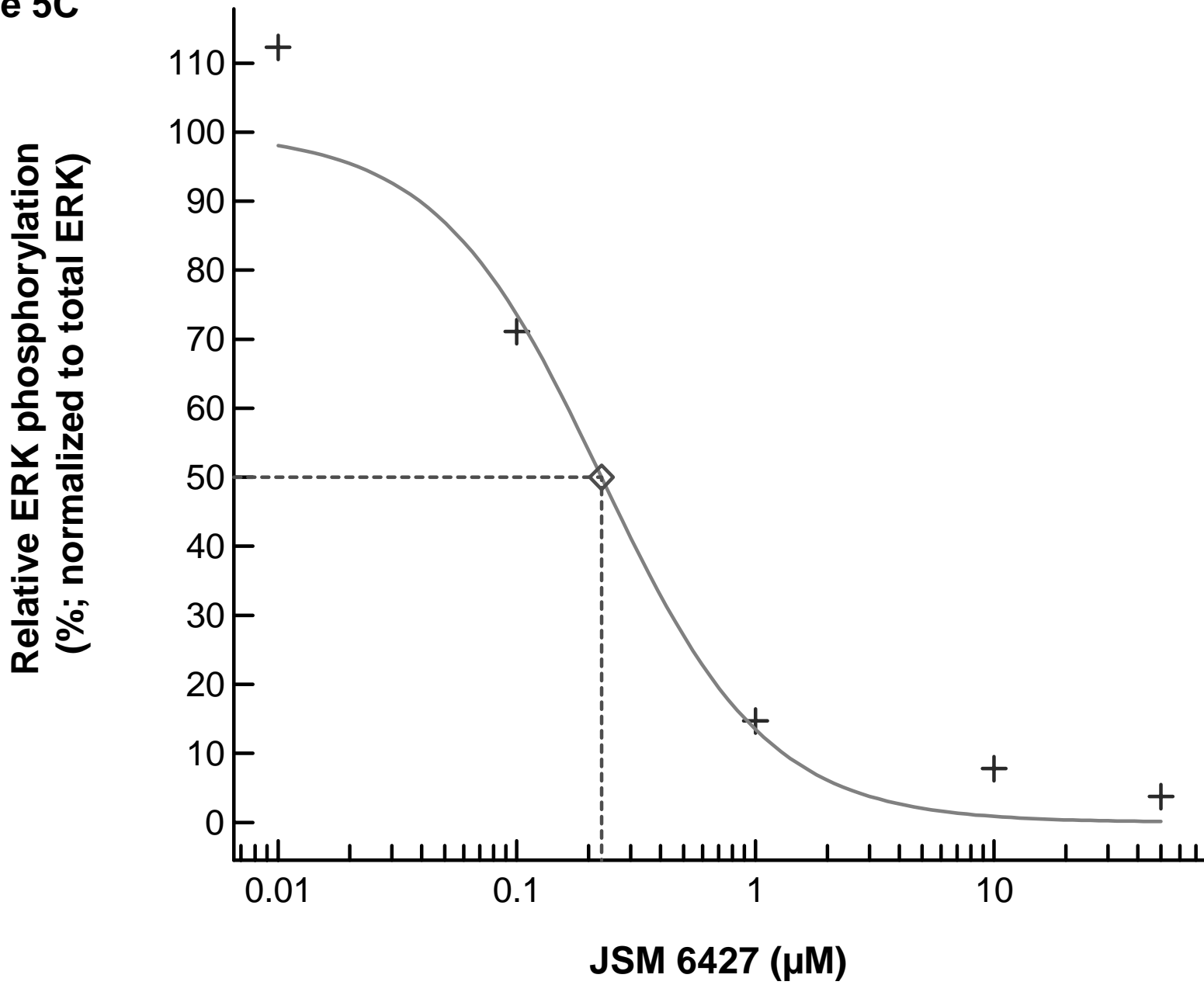




Figure 5C



**Figure 6**

